

TRITON
Algorithm Theoretical Basis
Document v2.0

Taiwan Space Agency
國 家 太 空 中 心

TABLE OF CONTENTS

1. Introduction.....3

2. Level 1a Calibration.....4

3. Level 1b Supporting Data Calculation.....7

4. Level 2 Products Retrieving.....9

5. Reference.....17

1 Introduction

This document mainly describes the detail of v2.0 TRITON data process system and products. Most of the content is similar to v1.0 data process (TRITON, 2024) and the different between v1.0 and v2.0 is also mentioned in this document. The four levels of TRITON v2.0 products, level 0, 1a, 1b, and 2, are similar to v1.0. The data levels can be corresponding to the product generation flow which is shown in Figure 1-1. The ellipses in Figure 1-1 are the name of algorithm and the squares are the data or products. The red and purple ellipses are indicated for data processing or system management. The description of data in each level and the correspondence to product generation flow is in below.

Level 0

The telemetry frames in Figure 1-1. The raw data down link from satellite. The format of Level 0 data is binary format and not be released.

Level 1a

The 11aDdm in Figure 1-1. The information in level 1a data is the raw data down link from satellite recorded in netCDF format.

Level 1b

The 11bDdm in Figure 1-1. The Level 1b CorDDM data is recorded in netCDF format and information in Level 1b CorDDM data is the same to level 1a and has been corrected the time shift occurs in receiver software. In Level 1b CorDDM data also record the calibrated DDM which remove the effect from the antenna and receiver.

The Supporting data in Figure 1-1. The Level 1b supporting data is recorded in netCDF format. The information in Level 1b metadata is the intermediate data calculated from Level 1b CorDDM data for further application. The main information in Level 1b metadata are the code phase and Doppler frequency of specular point (SP), effective scattering area, and normalized bistatic radar cross section (NBRCS) etc.

Level 2

The U10 and roughness in Figure 1-1. The retrieved ocean surface wind speed ($U_{10} < 20\text{m/s}$) and roughness (mean square slope and significant height) are recorded in Level 2 data.

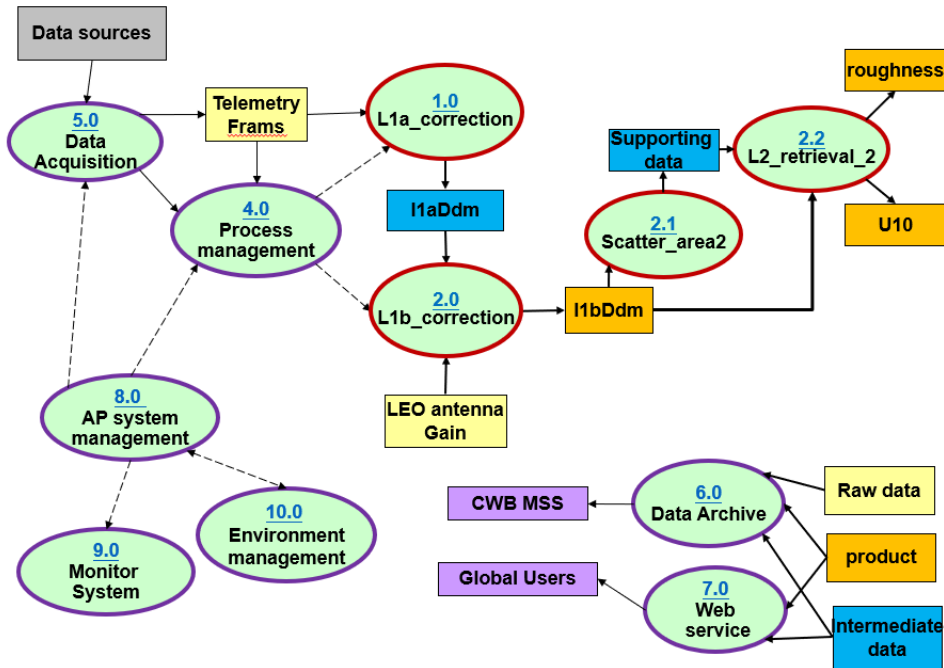


Figure 1-1 Product generation flow of TRITON mission.

2 Level 1a calibration

Due to the delay-Doppler map (DDM) is the signal strength of the received signal in different code phase delay and Doppler frequency, the signal strength is affected by the payload hardware. The level 1a calibration process is to derive the gain value of the payload to calculate the power of the received signal in different code phase delay and Doppler frequency.

The value of each bin in DDM can be described by

by

$$C = G(P_g + P_n + P_a + P_r), \quad (1)$$

where

C : the DDM values in counts

G : the total instrument gain applied to the incoming signal and noise in counts per watt

P_a : the thermal noise power received by the antenna in watts

P_g : the scattered signal power received by the instrument in watts

P_r : the thermal noise power generated by the instrument in watts

P_n : the noise power generated by the received signal with wrong PRN

$$P_a = k * T_a * B_w$$

$$P_r = k * T_r * B_w$$

k : Boltzmann's constant=1.380649e-23

T_a & T_r : antenna and receiver temperature

B_w : signal bandwidth

The noise floor C_n of DDM can be described by

$$C_n = G(P_n + P_a + P_r). \quad (2)$$

However, due to the P_n of each DDM is different, it needs to be removed to calculate G by

$$C_{min} = G(P_a + P_r), \quad (3)$$

then P_g can be derived by

$$P_g = (C - C_n) \frac{(P_a + P_r)}{C_{min}}. \quad (4)$$

C_{min} in (3) is derived by statistical method. Assume the relation between receiver and antenna temperature and noise floor is follow the equation

$$(noise\ floor, C_{min}) = a \times (antenna\ temperature) + b \times (receiver\ temperature) + c. \quad (5)$$

The process of C_{min} is illustrated in Figure 2-1. The first step of the process is to get the minimum noise floor of different antenna and receiver temperature. Then remove the data with less sampling. The relation between data sampling and minimum noise floor is shown in the right bottom panel in Figure 2-1. In the right bottom panel of Figure 2-1, the minimum noise floor with less sampling, which are indicated in black, are higher than with more sampling and are removed before analysis. The noise floor with less sampling before and after removing are shown in left top and right top panels in Figure 2-1, respectively. The second step is to remove the data too dispersed from the mean value of minimum noise floor. The data too dispersed from the mean value of minimum noise floor are indicated in light blue. The remaining data after first and second step are indicated in dark blue. The third step is to regress the remaining data by using (5). The regress results are indicated in red in the right bottom panel and also shown in the left bottom panel in Figure 2-1. The third step is to regress the coefficient a and b in (5). The coefficient c in (5) is calculated by using the noise floor measured from the payload when TRITON in the dormitory with fixed antenna and receiver temperature.

In second step, if the degree of dispersion for data removing is different, the regress result is also different. In order to determine the best coefficient of regression, nine different degree of dispersion is used for analysis. In v1.0 data process, the normalized bistatic radar cross section (NBRCS) module doesn't been ready, so the maximum value of DDM was used for comparison. In v2.0 data process, NBRCS is used for comparison with European Centre for Medium-Range Weather Forecasts (ECMWF) OSWS to calculate convergence degree. The comparison is shown in Figure 2-2. The convergence degree is calculated by counting the number of samples located in the center contour area in Figure 2-2 and shown in Figure 2-3. In Figure 2-3, the case 0 to 8 are the convergence degree of by using nine different degree of dispersion and case 9 is the convergence degree by using v1.0 coefficients. In Figure 2-3, case 4 has the maximum convergence degree, so the coefficients of case 4 are used for calibration.

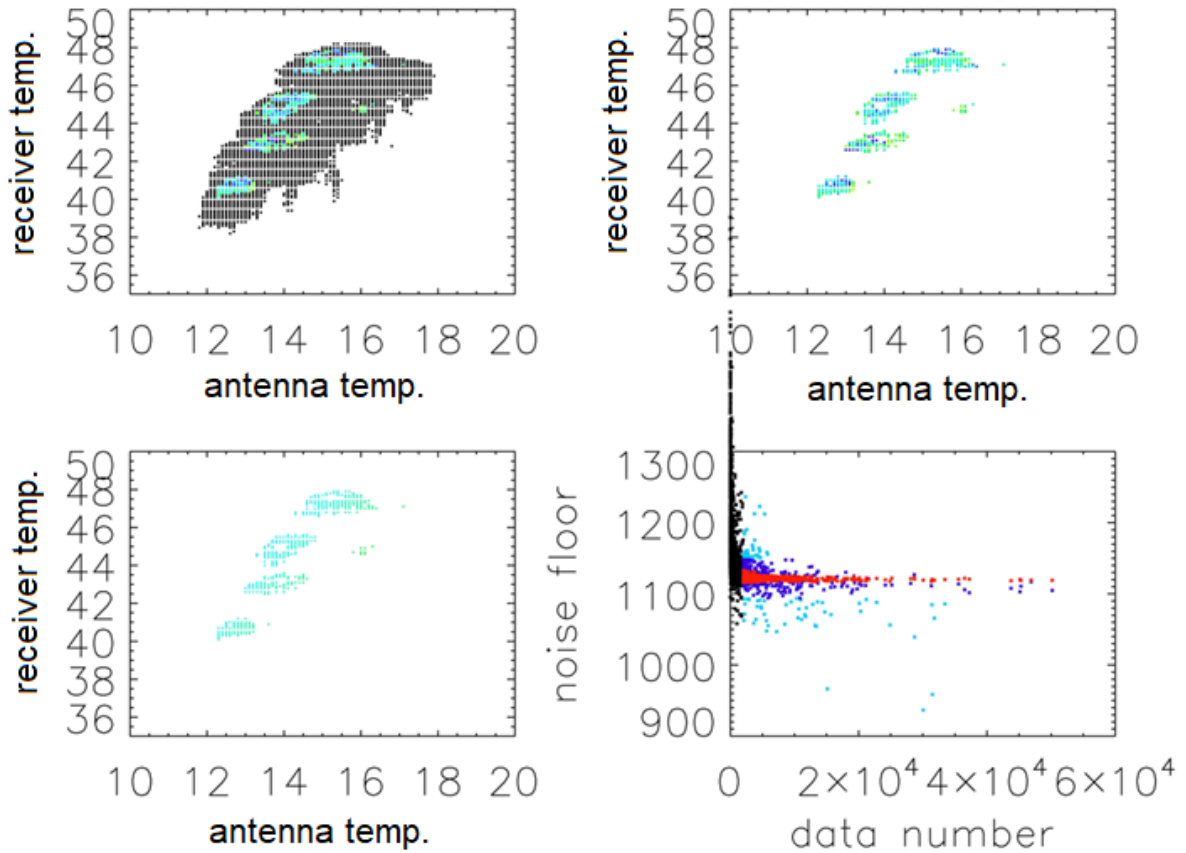


Figure 2-1 The illustration of C_{min} derivation in (3). Left top : the minimum noise floor in different antenna and receiver temperature. The color indicates the level of noise floor and black indicates the data not put into deriving process ; right top : the left top panel removes the black data ; left bottom : the regression result of the data in right top panel ; right bottom : the relation between data number and minimum noise floor. In right bottom panel, the black and light blue data are removed due to less sampling and too dispersed. The dark blue and red data are the data used for regression by (5) and the regression result.

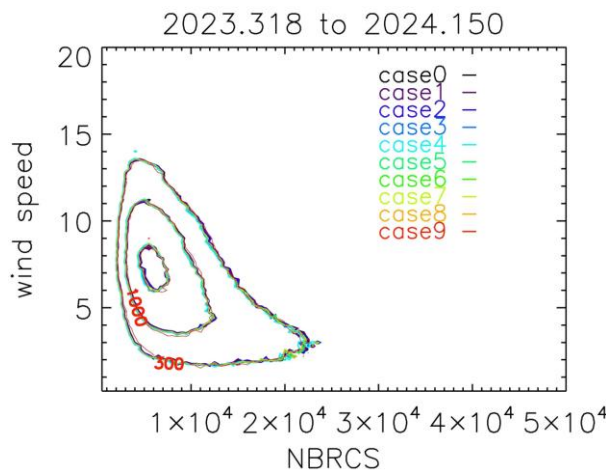


Figure 2-2 The comparison between NBRCS calculated by corrected DDM with different degree of dispersion removing for regression. The different degree of dispersion is indicated in different color.

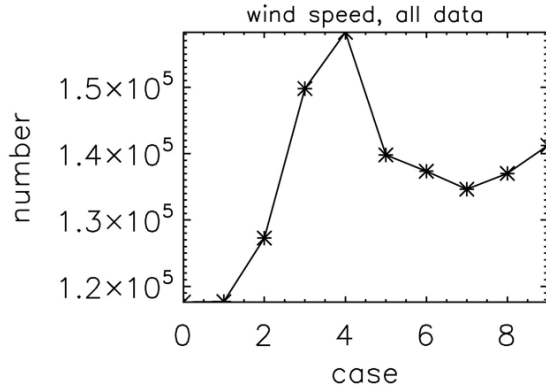


Figure 2-3 The NBRCS convergence degree of eight different cases by comparing with MSS (left), Hs (middle), and wind speed (right).

3 Level 1b supporting data calculation

Level 1b supporting data provides the intermediate data calculated from level 1b data. The main intermediate data is the code phase delay and Doppler frequency of SP and the NBRCS. In v1.0 data process, the code phase delay and Doppler frequency of SP is determined by comparing the shape of DDM and effective scattering area (ESA). The shape of ESA can be calculated by using the position and velocity of TRITON and GPS satellite. After calculating ESA, the relative position of SP in ESA is confirmed. Then slide the shape of ESA in different code phase delay and Doppler frequency and find the best matching result between ESA and DDM. Four matching results between ESA and DDM are shown in the top four panels and the contour comparisons between ESA and DDM are shown in the bottom four panels of Figure 3-1. In the bottom four panels of Figure 3-1, the yellow and blue asterisks are indicated the position of SPs determined from ESA comparison and positions of TRITON and GPS satellites, respectively. The position of yellow asterisks for SP position is more reasonable. However, if the signal to noise (SNR) of DDM is too weak, the determine result is not good enough. When the SNR of DDM too weak, world geodetic system 84 (WGS84) and DTU10 mean sea surface model are used for SP code phase and Doppler frequency determination in v2.0 data process.

The DDM theoretical model by Zavorotny and Voronovich (Z-V model) (Zavorotny and Voronovich, 2000) is

$$\langle P(\hat{\tau}, \hat{f}^D) \rangle = \frac{P^T \lambda^2}{(4\pi)^3} \iint_S \frac{G^T G^R}{R_0^2 R^2} \Lambda^2 \left(\frac{\delta \tau}{\tau_c} \right) S^2 \left(\frac{\delta f^D}{T_i} \right) \sigma_0 d^2 r \quad (6)$$

where $P(\hat{\tau}, \hat{f}^D)$ is the scattered signal power with different code phase delay $\hat{\tau}$ and Doppler frequency \hat{f}^D . And P^T , G^T , G^R , $\delta \tau$, δf^D , τ_c , T_i , S , r , R , R_0 , $\Lambda^2(\dots)S^2(\dots)$, and $\sigma_0(r)$ are GPS

satellite transmit power, GPS antenna gain at the specular point, receiver antenna gain at the specular point, the difference between the code phase delay of \hat{r} and $\hat{\tau}$, the difference between the Doppler frequency of \hat{r} and \hat{f}^D , chip, coherent integration time, the scattering surface, the point on the scattering surface, transmitter range from the scattering point, receiver range from the scattering point, WAF of pseudorandom C/A sequences, and normalized BRCS (NBRCS), respectively. (6) can be simplified as (CYGNSS, 2018)

$$\langle P(\hat{\tau}, \hat{f}^D) \rangle = \frac{P^T \lambda^2 G^T G^R \sigma_0 \bar{A}_{eff}}{(4\pi)^3 R_0^2 R^2} \quad (7)$$

where \bar{A}_{eff} is effective scattering area. Then NBRCS can be written as

$$\sigma_0 = \langle P(\hat{\tau}, \hat{f}^D) \rangle \frac{(4\pi)^3 R_0^2 R^2}{P^T G^T \lambda^2 G^R \bar{A}_{eff}}. \quad (8)$$

Due to the GPS satellite transmit power and GPS antenna gain cannot obtain immediately, these two terms are not be removed and the provided NBRCS are calculated as

$$P^T G^T \sigma_0 = \langle P(\hat{\tau}, \hat{f}^D) \rangle \frac{(4\pi)^3 R_0^2 R^2}{\lambda^2 G^R \bar{A}_{eff}}. \quad (9)$$

The three NBRCS calculated by using three different bin number, 1×1 , 3×5 , and 13×21 with the SP bin located in center, are provided. The illustrations of three area with three different bin number in DDM and ESA are shown in Figure 3-2.

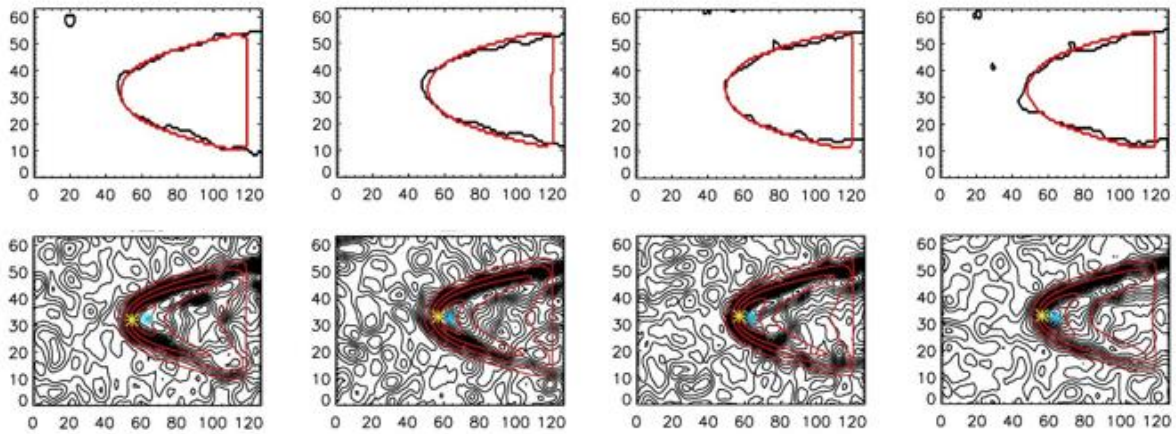


Figure 3-1 Top : Matching results between ESA and DDM. Bottom : Contour comparisons between ESA (red) and DDM (black). The yellow and blue asterisks are indicated the position of SPs determined from ESA comparison and positions of TRITON and GPS satellites, respectively.

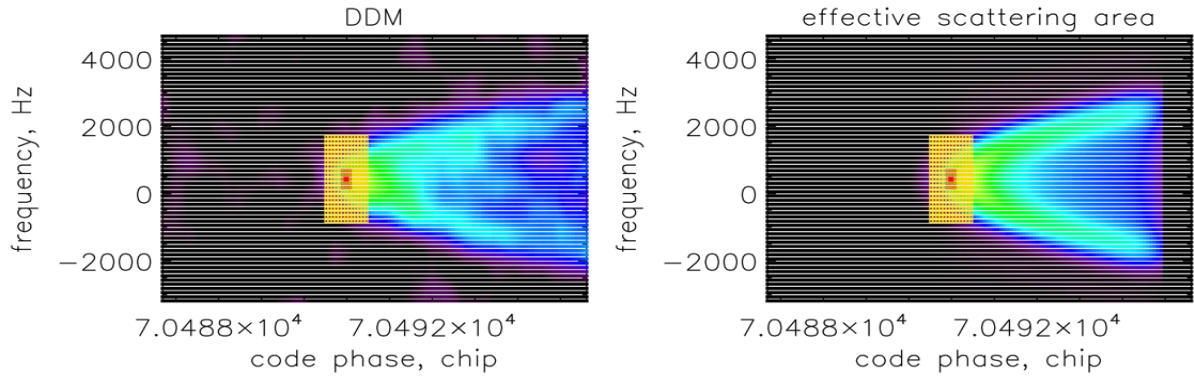


Figure 3-2 Illustration of three different bin number, 1×1 , 3×5 , and 13×21 with the SP bin located in center in DDM (left) and ESA (right). The area of 1×1 , 3×5 , and 13×21 are indicated by red dot, red rectangle, and yellow rectangle.

4 Level 2 products retrieving

TRITON satellite mission has three level 2 products, OSWS, MSS, and Hs.

The mean square slope (MSS) and significant height (Hs) are similar to v1.0 and is not described in this document.

The OSWS is retrieved by geophysical model function (GMF). The GMF for OSWS is derived from the comparison between NBRCS and European Centre for Medium-Range Weather Forecasts (ECMWF) OSWS. In v1.0 data process, DDM with all prn GPS satellite is used for different signal incident angle classification. In v2.0 data process, each prn GPS satellite, the signal incident angle, and the azimuth angle of satellite velocity of TRITON and GPS satellites are used for classification and correction, respectively.

For the satellites velocity azimuth angle correction, calculate the difference between the NBRCS in different relative velocity between TRITON and GPS satellites and then correct the difference when before retrieving. The GMF before and after correction for different GPS blocks and NBRCS calculated by using different number bins are shown in Figure 4-1 and 4-2, respectively. The data convergence after correction (Figure 4-1) is better than before correction (Figure 4-1).

The comparisons between NBRCS after correction and ECMWF OSWS for each prn GPS satellite are used for GMF development. The comparisons for example are shown in Figure 4-3. In Figure 4-3, the yellow dots and red dots are the average NBRCS with different OSWS and average OSWS with different NBRCS. The yellow and red dots are used to develop GMF by using the equations

$$NBRCS = a_1(U10_1)^{-2} + b_1(U10_1)^{-1} + c_1 \quad (10)$$

and

$$U10_2 = a_2(NBRCS)^{-2} + b_2(NBRCS)^{-1} + c_2, \quad (11)$$

respectively. The results for example are shown in Figure 4-4. In Figure 4-4, The black and red dots are the average NBRCS with different OSWS and average OSWS with different NBRCS,

 TASA 國家太空中心 Taiwan Space Agency	TRITON Algorithm Theoretical Basis Document v2.0	
		10 OF 17

respectively. The red and green lines are the developed GMFs by using black and red dots, respectively. Noted that the equations of GMF for v1.0 are

$$NBRCS = a_1 (U10_{1,v1.0})^{-3} + b_1 (U10_{1,v1.0})^{-2} + c_1 (U10_{1,v1.0})^{-1} + d_1 \quad (12)$$

and

$$U10_{2,v1.0} = a_2 (NBRCS)^{-3} + b_2 (NBRCS)^{-2} + c_2 (NBRCS)^{-1} + d_2. \quad (13)$$

Two GMFs are used for OSWS retrieving. In v1.0 data process, the average of $U10_{1,v1.0}$ and $U10_{2,v1.0}$ in (12) and (13), respectively, is the final retrieval OSWS. In v2.0, for OSWS larger around 5m/s, only $U10_1$ in (10) is the final retrieval OSWS. For OSWS less than around 5m/s, the final retrieval result OSWS is $w_1 \times U10_1 + w_2 \times U10_2$, where w_1 and w_2 are the weighting coefficients. The value of w_1 and w_2 are different with different NBRCS, different signal incident angle, and different prn GPS satellites. The comparisons between retrieval OSWS and ECMWF OSWS are shown in Figure 4-5. The root mean square error (RMSE) of retrieval OSWS is around 2.25m/s. Compare with the RMSE of v1.0 retrieval OSWS is around 2.65m/s, where the comparisons between v1.0 retrieval OSWS and ECMWF OSWS are shown in Figure 4-6, v2.0 retrieval OSWS is better than v1.0 for around 0.4m/s.

The preliminary high OSWS also provided in v2.0 product. The high OSWS is retrieved by using the High-resolution tropical cyclone nature run. One example of the relative positions of simulated typhoon and TRITON SP is shown in Figure 4-7. Three simulated typhoon OSWS are used for comparing with NBRCS. The comparisons are shown in Figure 4-8. In Figure 4-8, not only the comparison between NBRCS and simulated typhoon OSWS but also the comparison between NBRCS and ECMWF OSWS are plotted together for comparisons. The red and black dots are the comparisons between NBRCS with simulated typhoon OSWS and NBRCS with ECMWF OSWS. The yellow and green dots are the average NBRCS with different OSWS and average OSWS with different NBRCS, respectively. The corresponding simulated typhoon OSWS to TRITON SP can up to around 40m/s which is high than the maximum OSWS of ECMWF. The comparisons between NBRCS and simulated typhoon OSWS are used for GMF development. Due to the corresponding observation in simulated typhoon area is not enough for prn and signal incident angle classifications. The developed GMF by different bins for NBRCS calculations are shown in Figure 4-9. The colored dots are the data density. The two yellow curves are the two GMF developed by using the yellow and green curves in Figure 4-8. The comparisons between retrieval and ECMWF OSWS are shown in Figure 4-10. Due to the data is not enough for classifications and the developed GMFs are for all prn GPS satellite and all signal incident angle, the RMSE is around 3.5m/s, which is higher than normal retrieval OSWS.

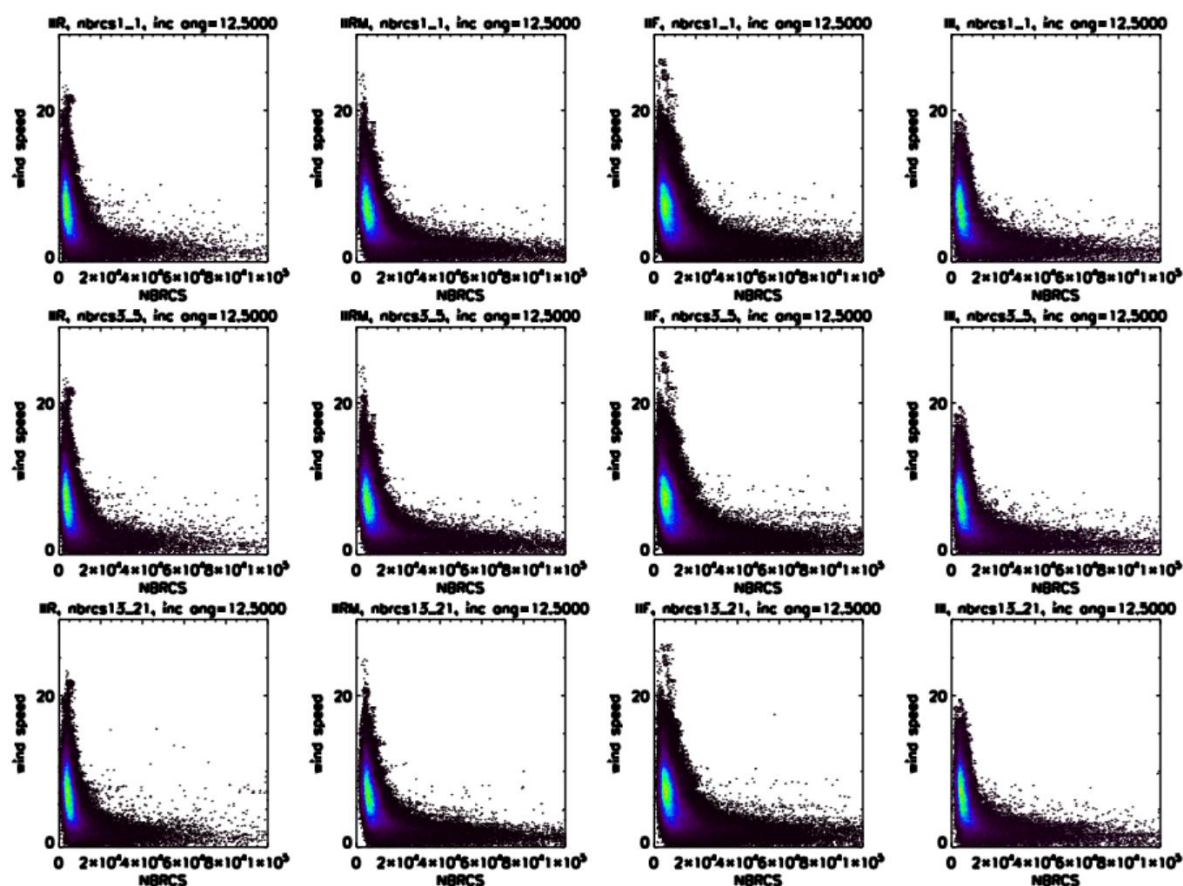


Figure 4-1 Comparisons between ECMWF OSWS and NBRCS before satellite velocity azimuth angle correction with different blocks and bins usage. (left to right) IIR, IIRM, IIF, and III blocks. (top to bottom) NBRCS calculation by using 1×1 , 3×5 , 13×21 bins of DDM.

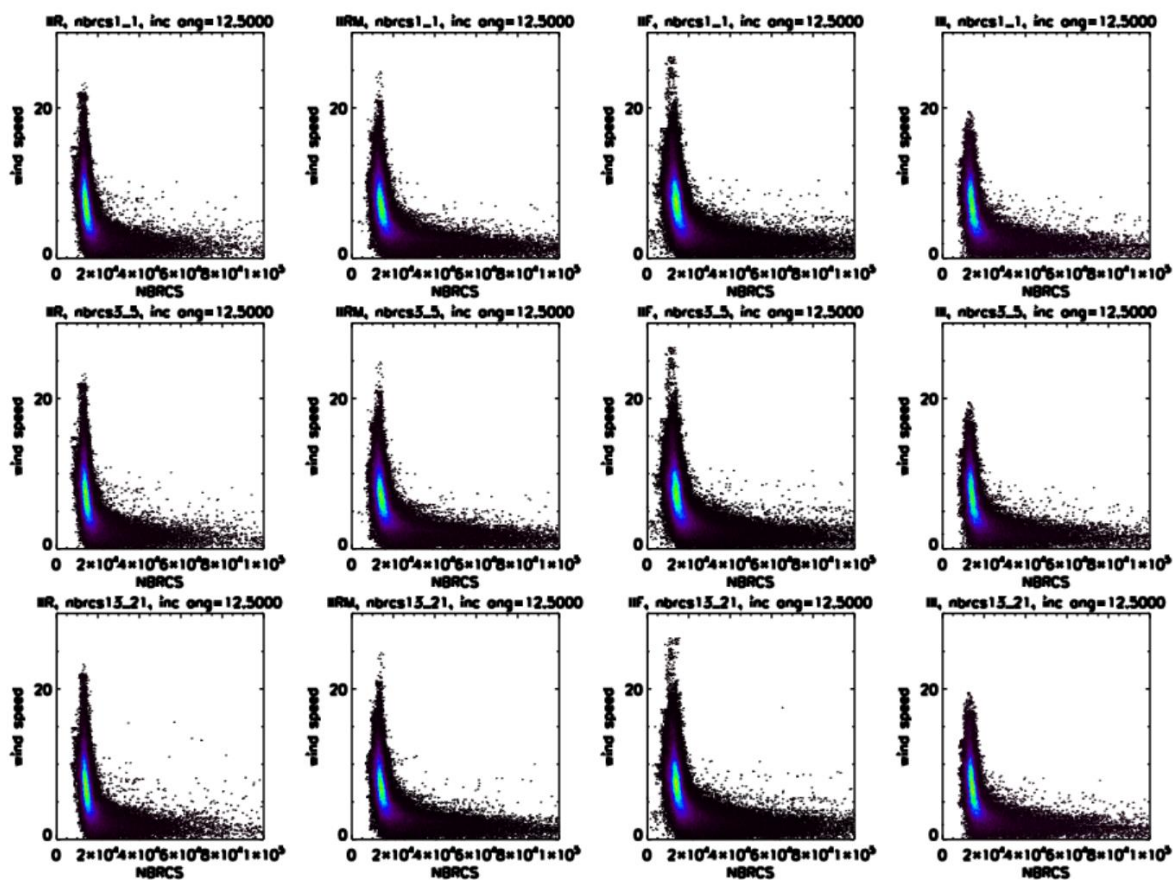


Figure 4-2 Comparisons between ECMWF OSWS and NBRCS after satellite velocity azimuth angle correction with different blocks and bins usage. (left to right) IIR, IIRM, IIF, and III blocks. (top to bottom) NBRCS calculation by using 1×1 , 3×5 , 13×21 bins of DDM.

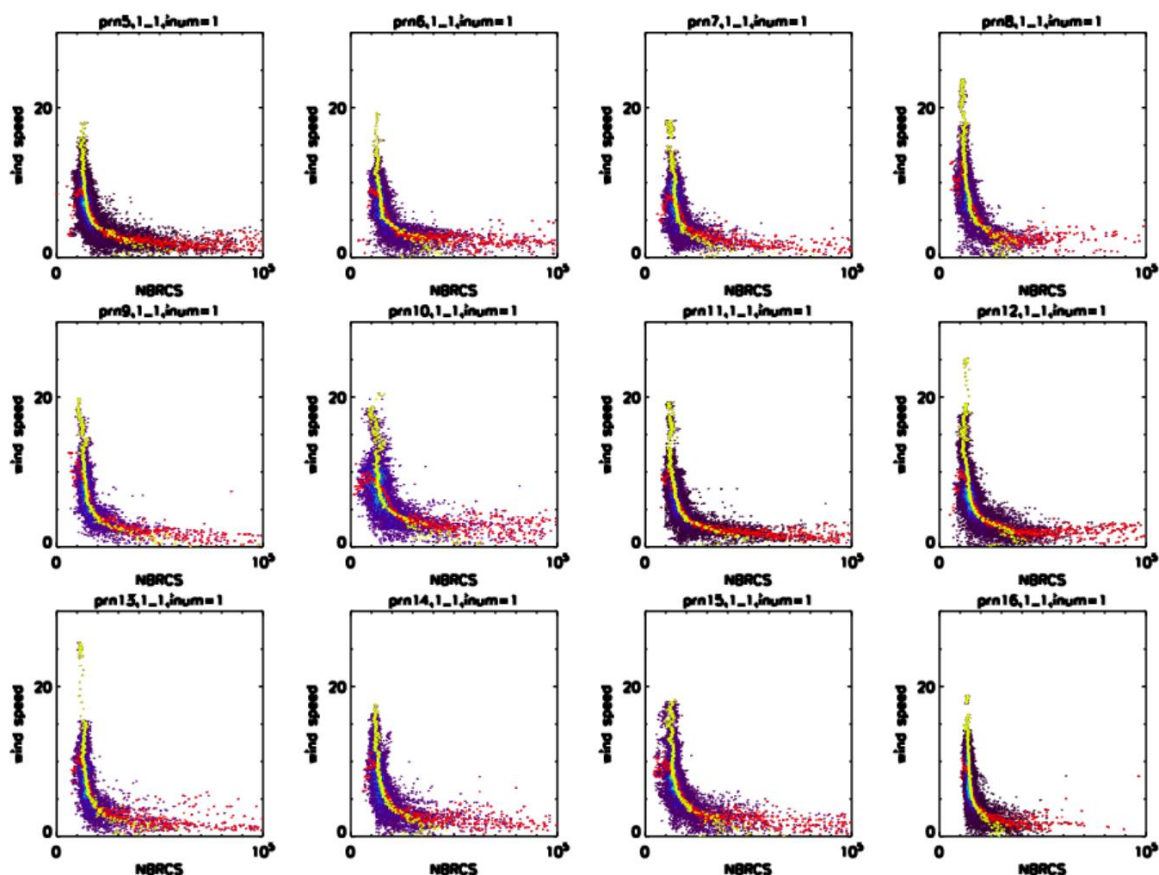


Figure 4-3 Comparison between NBRCS after satellite velocity azimuth correction and ECMWF OSWS of prn 5 to 16 satellites when signal incident angle between 5 to 10 degree. The yellow dots and red dots are the average NBRCS with different OSWS and average OSWS with different NBRCS, respectively.

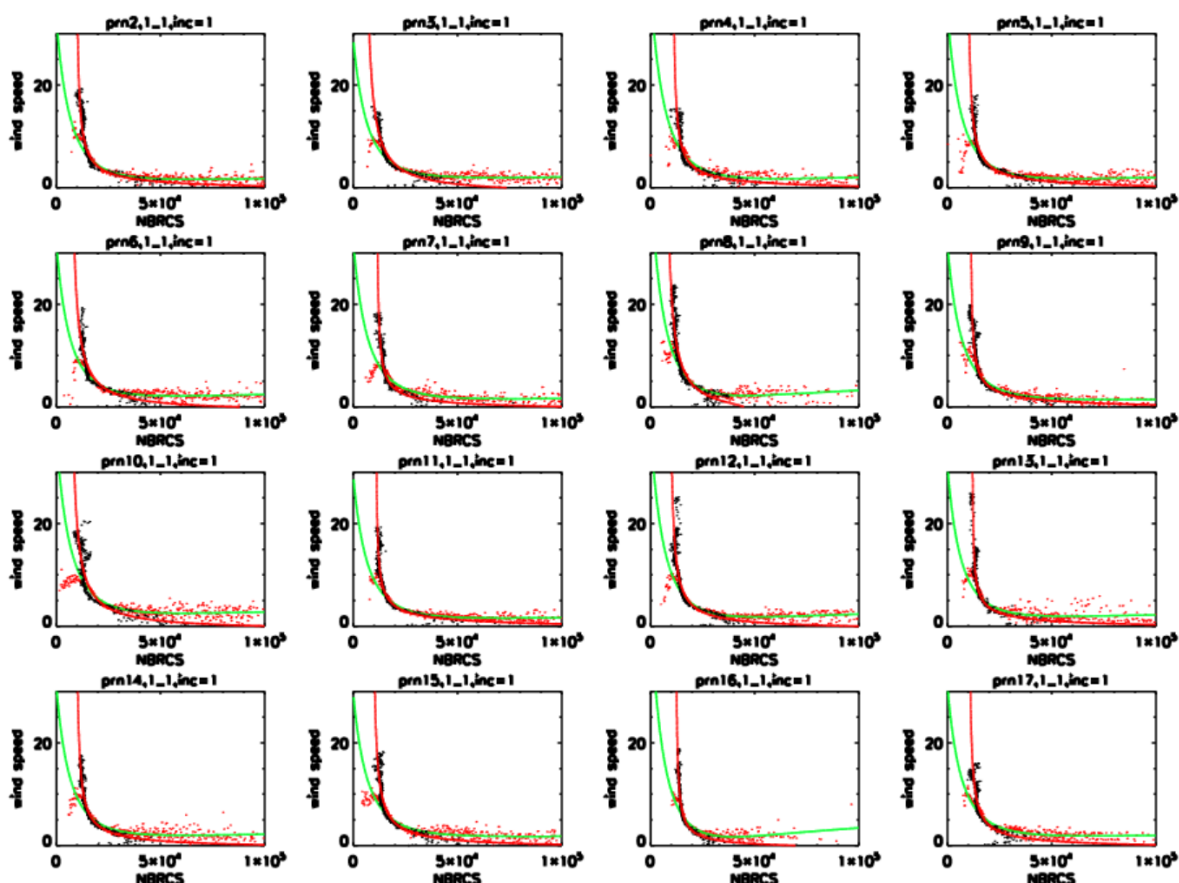


Figure 4-4 GMF development. The black and red dots are the average NBRCS with different OSWS and average OSWS with different NBRCS, respectively. The red and green lines are the developed GMFs by using black and red dots, respectively.

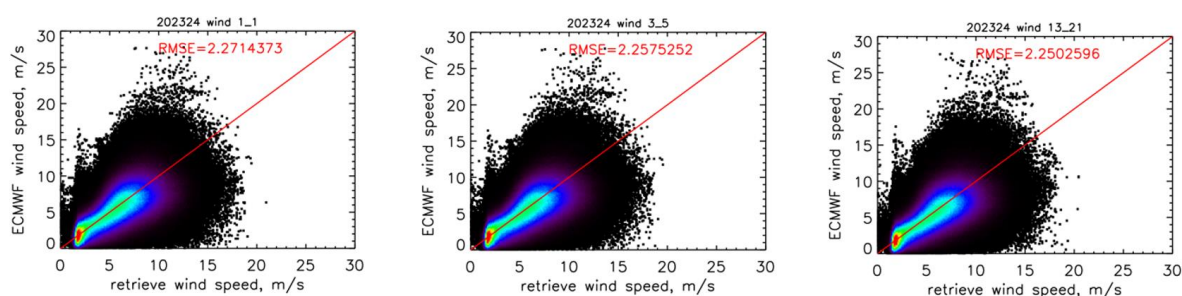


Figure 4-5 Comparisons between retrieval OSWS and ECMWF OSWS by using TRITON data from day of year 2023.318 to 2024.366. The RMSE are around 2.25m/s. (left to right) the retrieval OSWS by using 1×1 , 3×5 , 13×21 bins of DDM.

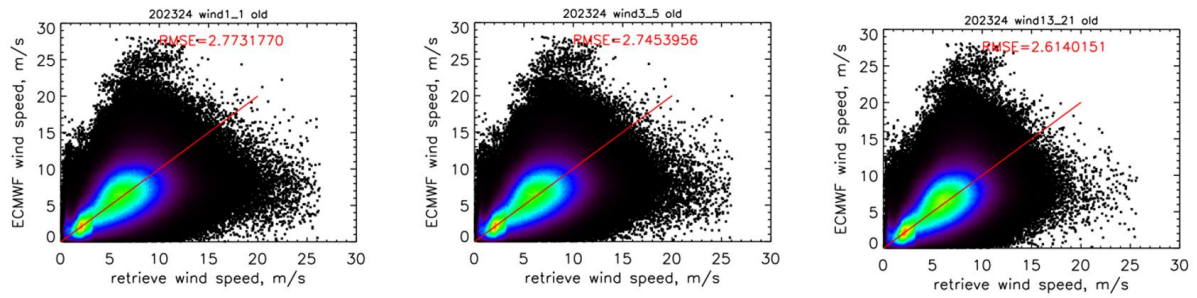


Figure 4-6 Comparisons between v1.0 retrieval OSWS and ECMWF OSWS by using TRITON data from day of year 2023.318 to 2024.366. The RMSE are around 2.65m/s. (left to right) the retrieval OSWS by using 1×1 , 3×5 , 13×21 bins of DDM.

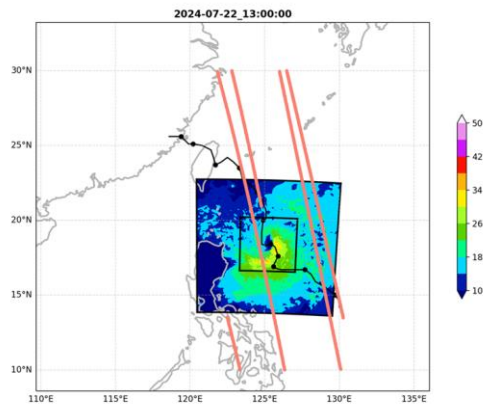


Figure 4-7 Comparison between simulated **typhoon** and SP of TRITON observation, for example. The color of colored area indicates the typhoon OSWS in simulated area. The red lines are the SP of TRITON observation.

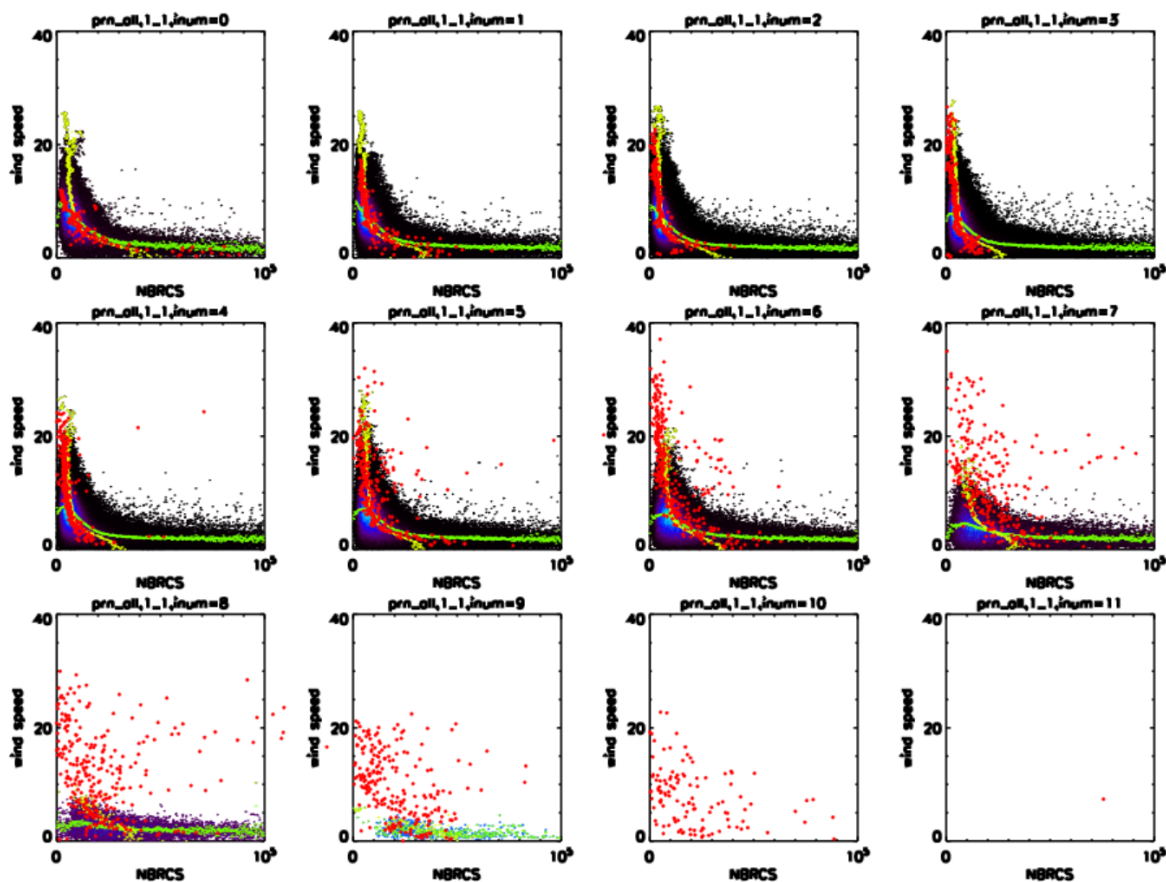


Figure 4-8 The comparisons between NBRCS, simulated typhoon OSWS, and ECMWF OSWS. The red dots are the comparison between the NBRCS and simulated typhoon OSWS. The block dots are the comparison between NBRCS and ECMWF OSWS. The yellow and green dots are the average NBRCS with different OSWS and average OSWS with different NBRCS, respectively.

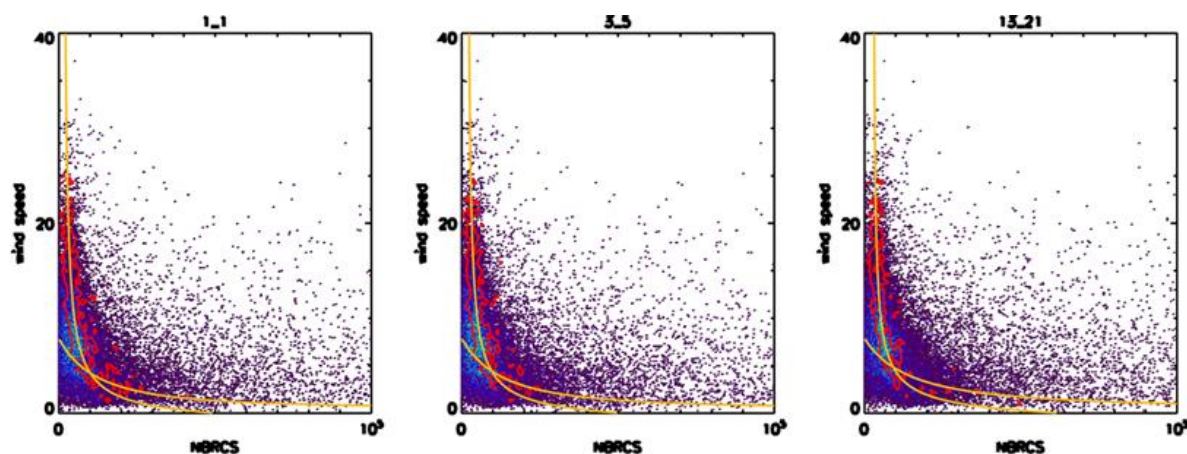


Figure 4-9 The comparisons between BRCS and GMFs.

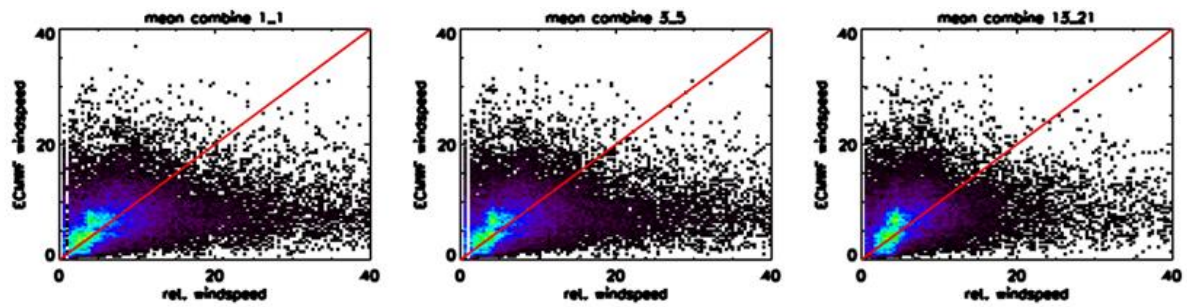


Figure 4-10 Comparisons between retrieval and ECMWF OSWS by using 1×1 , 3×5 , 13×21 bins of DDM (from left to right).

5 Reference

Zavorotny, V, Voronovich A (2000) Scattering of GPS signals from the ocean with wind remote sensing applications. IEEE Trans. Geosci. Remote Sens. 38(2): 951–964.

CYGNSS (2016) Algorithm Theoretical Basis Document Level 2 Mean-Square Slope Retrieval.

CYGNSS (2018) Algorithm Theoretical Basis Document Level 1B DDM Calibration.

TRITON (2024) Algorithm Theoretical Basis Document v1.0.